PHYSICAL REVIEW B VOLUME 36, NUMBER 5 15 AUGUST 1987-I

Electron gas in channels in strong magnetic fields

S. T. Chui
Bartol Research Foundation of the Franklin Institute at University of Delaware, Newark, Delaware 19716
(Received 22 October 1986; revised manuscript received 7 November 1986)

The physics of an electron gas in a strong magnetic field in channel geometries is discussed. For very narrow channels, the electrons form a one-dimensional (1D) "Fermi sea" with a concomitant $2k_F$ charge-density-wave (CDW) instability. For a 1D spinless electron gas in the absence of a magnetic field, there is usually a competition between the "superconducting" and CDW instabilities so that the CDW instability does not occur. Because of the spatial dependence of the exchange interaction in the effective 1D Hamiltonian in the present case, the conventional cancellation between these instabilities becomes incomplete and a CDW instability results. The transition from a one-dimensional "Fermi sea" with a $2k_F$ CDW instability to a two-dimensional situation which exhibits the fractional quantized Hall effect as the channel width is increased is investigated. As the width is increased, except under some special circumstances that correspond to odd-denominator filling factors when the gap is not changed much, the gap in the excitation spectrum undergoes a damped oscillation. We interpret the oscillation in terms of the formation of clusters due to multiparticle exchange and its breakup.

I. INTRODUCTION

A strong external magnetic field induces many interesting phenomena. In the fractional quantized Hall effect (FQHE),[1] one studies the physics of a two-dimensional (2D) electron gas. One-dimensional (1D) channel structures as narrow as 100 Å on heterojunctions and on metal-oxide-semiconductor-field-effect-transistors MOSFET's (Ref. 2) are becoming available experimentally. We have recently investigated the physics in these 1D channels and found that[3] if the channel width is narrow enough, a gap exists in the excitation spectrum for even as well as for odd-denominator filling factors. In the 2D case, a gap exists in the excitation spectrum only for odd-denominator filling factors. In this paper we first reexamine the situation when the channel width is very narrow under the more realistic hard wall boundary conditions; we then investigate how the 2D limit is approached as the channel width is increased.

A more precise reinterpretation of our results for very narrow channels suggest the formation of a 1D "Fermi sea" of the electrons. In addition, the density autocorrelation function exhibits a peak at momentum transfer $2k_F$, indicating a charge-density-wave (CDW) instability. Because of the resemblence of the ground state to the 1D "Fermi sea", we investigate the applicability of the 1D renormalization-group (RG) perturbation calculations. For a 1D spinless electron gas in the absence of the magnetic field, there is usually a competition between the superconducting and CDW instabilities so that the CDW instability does not occur.[5] Because of the momentum dependence of the e-e interaction in the effective 1D Hamiltonian in the present case, the conventional cancellation between these channels becomes incomplete. The novel physics of this incomplete cancellation has not been discussed previously. The FQHE is also thought to be intimately related to the effect of multiparticle exchange.[4,6] The competing diagrams in the RG calculation can be considered to correspond to exchange processes. In this sense our results for the narrow channels and the FQHE are connected.

The single particle states of an electron in a magnetic field can be characterized by its average x position (y momentum). The "Fermi sea" which exists for very narrow channels consists of a single cluster such that every contiguous state with neighboring y momenta (x positions) is occupied. As the width of the channel is increased; if the electrons were to still form a single cluster, its effective size has to increase. Because of the finite range of the multiparticle exchange, when the cluster gets large, the exchange cannot completely counterbalance the direct Coulomb repulsion; the cluster becomes unstable and breaks up.[4] This is observed in our finite cluster calculations. We find that the gap in the excitation spectrum decreases to zero because of the fluctuation between configurations with different number of clusters and then becomes finite again when the two cluster configuration becomes stable. Presumably it undergoes a damped oscillation as more and more clusters are formed. We now describe our calculation in detail.

II. THE HAMILTOIAN

We first express the Coulomb potential in terms of the single particle basis states of electrons in a magnetic field in channels. The single particle wave function can be characterized by states similar to the Landau orbitals. We have to incorporate the effect of the boundary conditions (BC's), however. To impose the hard-wall BC across the channel it is easier mathematically to pick the y axis along the channel. The eigenfunctions can then be written as[7]

$$\phi_j(\mathbf{r})=\exp(ik_j y)f(x)/(L_y)^{1/2} \quad (1)$$

where $k_j=(L_x/N_s)j$ and

$$f''-(k-x)^2f+ef=0 \tag{2}$$

$e=2mE/\hbar^2$, N_s is the total number of single-particle basis states in the system. We have imposed periodic boundary conditions along the channel since it is usually long compared with the magnetic length. $f(0)=f(L_x)=0$ from the hard-wall BC across the channel. f can be expressed in terms of the Weber functions.[8] However, it is computationally more convenient to directly integrate the differential equation numerically. With a sixth order Runge-Kutta differential equation solver that adjusts its step size automatically to satisfy the imposed error condition, we obtained the eigenvalue $e(k)$ illustrated in Fig. 1 for different channel widths as a function of the distance k measured with respect to one edge. The eigenvalue of the dimensionless equation reduces to the free-particle value $(2n+1)$ when the channel width, L_x, is infinite. For channel widths larger than 3.55, the eigenvalue for different channel lengths forms a single curve. The effect of the other edge is exponentially small. When k reaches the channel edges, the energy E is equal to $1.5\hbar\omega_c$, the energy of the next Landau level. Hence k has to be inside the channel or the next Landau level will start getting filled. Thus even though the single particle spectrum is continuous and well defined even for k outside the channel in the limit that the channel length becomes infinitely long, the filling factor is still a precisely defined quantity. In the following we shall thus call the filling factor the quantity $A/(2\pi N)$ where A is the area of the channel and N is the total number of electrons.

The Hamiltonian can be written as

$$H=\sum_{[j]} A(j_1,j_2,j_3,j_4)C^\dagger_{j_1}C^\dagger_{j_2}C_{j_3}C_{j_4}+\sum_k e(k)C^\dagger_kC_k. \tag{3}$$

The A's are integrals of the Coulomb potential and the orbitals ϕ_j's given by

$$A=\frac{e^2}{2l^2L_y}\int_{q_x}\delta(j_1+j_2=j_3+j_4)\,|\mathbf{q}|^{-1} \times\langle j_1|\exp(i\mathbf{q}\cdot\mathbf{r})|j_4\rangle \times\langle j_2|\exp(-i\mathbf{q}\cdot\mathbf{r}')|j_3\rangle. \tag{4}$$

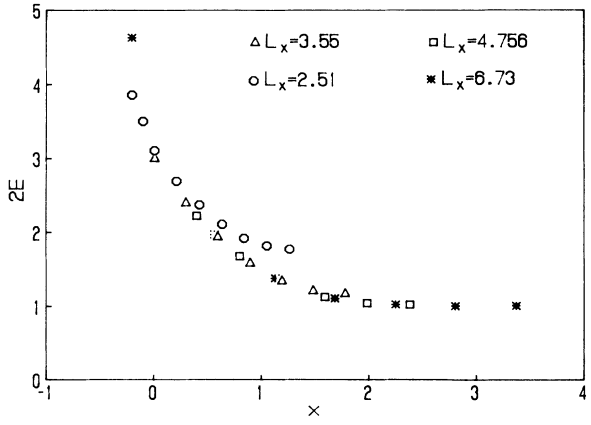

FIG. 1. The eigenvalues of the electron in a magnetic field under hard wall [Eq. (2)] boundary conditions as a function of its y-momentum k measured from the hard wall for channel widths $L_x=2.51$, open circles, 3.55, open triangles, 4.76, open squares, 6.73, asterisk. Due to overcrowding, some data points at small x and large L_x have not been shown.

The integral $\langle j_1|\exp(i\mathbf{q}\cdot\mathbf{r})|j_4\rangle$ has been carried out numerically. We have picked different mesh sizes r and found that, except for the constant diagonal term which does not affect the excitation spectrum,[9] the convergence is very fast.

We have compared these matrix elements with those obtained using the free particle Landau wave functions in place of the ϕ_j. The two types of matrix elements are approximately the same. When the index j is close to the wall boundary, the matrix elements for the finite channels are usually larger than the free results because the "hard-wall" wave function, squeezed in by the walls, have not moved away as much.

The matrix element A is not a function of the momentum transfer $q_y=j_2-j_3$ alone. This makes the Hamiltonian different from the conventional 1D Hamiltonian $H'=\sum_{q_y}\bar{V}(q_y)\bar{\rho}(q_y)\bar{\rho}(-q_y)$ where the 1D density operator $\bar{\rho}$ is given by $\bar{\rho}(q_y)=\sum_j C^\dagger_{j+q_y}C_j$. This momentum dependence causes an incomplete cancellation of the "Cooper channel" and the "zero sound channel" diagrams.

III. NARROW CHANNEL REVISITED

The Hamiltonian matrix of four-, six-, and eight-electron systems have been diagonalized for $\hbar\omega_c/(e^2/\varepsilon l)=r=1$ and 3, approximately the experimental situation. For the "half-filled" case and $L_x=4.76$, the two lowest eigenstates occur with total y- momenta J that differ by 1. For $r=3$, the gap in the excitation spectrum is equal to 0.55, 0.44, and 0.42 for $N_s=9$, 13 and 17 respectively. (N_s is odd so that the two ends are both on the boundary of the wall.) From extrapolation, we estimate the gap to be $0.41e^2/\varepsilon l$. We have experimented with including states with their k's outside the channel for the case of six electrons and found that they are weakly coupled to the low-lying states; the final results are unaffected by it. For $r=1$, the gap is equal to 0.28, 0.24, and 0.26 for $N_s=9$, 13, and 17 respectively.

The ground-state wave function $|0\rangle$ turns out to be very simple. Even though there are many (88 for $N_s=13$ and $J=39$) basis functions, significant contributions to it comes from only a few states. This is shown in Fig. 2 for the case with $r=1$. For $N_s=9$, the lowest state has $J=22$ and correspond to [4,5,6,7] occupied. For $N_s=13$, the lowest energy state has $J=39$ and corresponds to the cluster [4,5,6,7,8,9] occupied with small fluctuations about it. The ground state is like a "Fermi sea" such that all states with y momentum from $-k_F$ (4) to k_F (9) are occupied. This cluster seems to form as a consequence of the

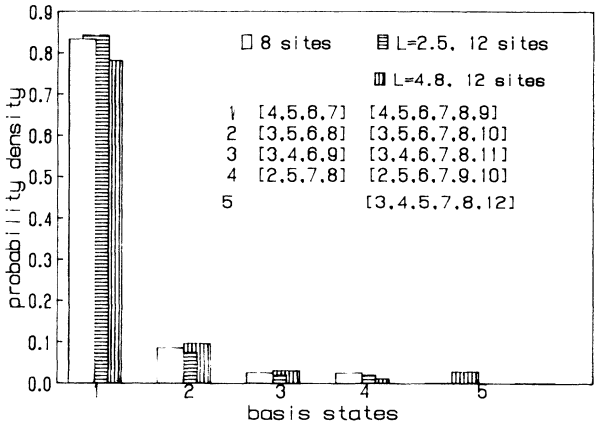

FIG. 2. The probability density of the ground-state wave function.

combined effects of the attractive multiparticle exchange[4] caused by the overlap in the x direction and of the compression caused by the walls. Because the electrons are Fermions, they cannot occupy states with the same quantum number. Instead, they try to stay as close to each other in the x direction as is possible. Normally, there is a kinetic energy cost in keeping particles close to each other. Because of the magnetic field, this kinetic energy cost is absent in the present case.

In addition, all the other significant contribution to the ground-state wave function corresponds to a CDW density modulation with $q_y = 2k_F$. For example, for $N_s = 13$ the state [3,5,6,7,8,10] corresponds to electrons excited from 4 to 10 and from 9 to 3 with momentum transfer $\pm 2k_F \cong 6$. [3,4,6,7,8,11] corresponds to 5 to 11 and 9 to 3; [2,5,6,7,9,10] corresponds to 4 to 10 and 8 to 2; [3,4,5,7,8,12] corresponds to 6 to 12 and 8 to 2. This $2k_F$ density modulation is consistent with our previous calculation[3] with a different boundary condition. Because of the indistinguishability of the particles, the above states also provide a contribution to the density autocorrelation function at small momentum transfers. Thus 4 to 10 and 9 to 3 can also be interpreted as 4 to 3 and 9 to 10 with a momentum transfer of 1. These small momenta transfers are different for the different states (1,2,2,3). In contrast to the $2k_F$ contribution, they do not add coherently.

A similar ground state is also observed at $N_s = 9$. Thus the Fermi sea is [4,5,6,7] whereas the excited state [3,5,6,8] corresponds to electrons excited from 7 to 3 and 4 to 8; [3,4,6,9] corresponds to 7 to 3 and 5 to 9; [2,5,7,8] corresponds to 6 to 2 and 4 to 8.

The CDW instability also exhibits a finite q_x dependence in our numerical calculation. The amplitude of the different contributions to the wave function is not all of the same sign. The 2D density operator ρ is given by

$$\rho(q_y,q_x) = \sum_j \exp[-q^2/2 + iq_x(j+q_y/2)] \times C^{\dagger}_{j+q_y} C_j .$$

For $N_s = 9$, the ground-state wave function is

$$|0\rangle = -0.949\,|1\rangle + 0.258\,|2\rangle - 0.115\,|3\rangle - 0.104\,|4\rangle .$$

All these states provide a coherent contribution to the density autocorrelation function at $q_x \cong \pi$ and $q_y = 2k_F$. Similarly for $N_s = 13$, the ground state wave function at $r = 1$ is

$$|0\rangle = 0.884\,|1\rangle - 0.31\,|2\rangle + 0.177\,|3\rangle + 0.168\,|4\rangle - 0.107\,|5\rangle . \quad (5)$$

This exhibits a density modulation at $q_x \cong \pi$ and $q_y = 2k_F$. The ratio q_y/q_x at which the density autocorrelation function peaks is approximately equal to 2. The period in r space of the charge density fluctuation in the x direction is thus twice as big as that in the y direction. This suggests the physical picture such that the electron exhibits a tendency to lump at equal y distance along the channel and, in addition, move up and down to avoid each other as one goes down the channel.

In addition to the exchange, the influence of the walls comes in to further stabilize the single cluster configuration. We have performed a finite cluster calculation for $L_x = 4.7$ for 13 sites for which all the single-particle site energies are the same. The resulting ground-state wave function exhibits a much larger fluctuation.

Our numerical calculation demonstrates a tendency towards the formation of a CDW. It does not show that there is true long-range order in the CDW for the ground state. The fact that we see a gap in the excitation spectrum combined with Goldstone's theorem suggests that the long-range order is at most algebraic.

The excited state is dominated by the configuration that consists of the ground state but with the boundary site displaced outward by one unit, i.e., [4,5,6,7,8,10]. For example, for $L_x = 4.76$, $N_s = 12$, and $J = 40$, the lowest state has its amplitude concentrated among a few of the 90 basis states. For $r = 3$, 1 this is equal to

$$0.965\,|4,5,6,7,8,10\rangle - 0.194\,|3,5,6,7,9,10\rangle - 0.123\,|3,5,6,7,8,11\rangle$$

and

$$|1\rangle = 0.839\,|4,5,6,7,8,10\rangle - 0.343\,|3,5,6,7,9,10\rangle - 0.238\,|3,5,6,7,8,11\rangle + 0.115\,|3,4,6,7,9,11\rangle + 0.12\,|3,4,6,7,8,12\rangle + 0.18\,|2,5,6,8,9,10\rangle , \quad (6)$$

respectively. Equations (5) and (6) are approximately related by $|1\rangle \cong \bar{\rho}(q_y = 1)\,|0\rangle$. In the limit that the channel length becomes long, we expect the excited state will consist of density fluctuations of the form $\bar{\rho}(q)\,|0\rangle$.

While our wave function shows a connection with the noninteracting ground state, there are differences. First of all, the $2k_F$ instability that we discuss is absent in the noninteracting ground state. Secondly, as the cluster size N_s is increased, the energy difference between the noninteracting ground and first excited state goes to zero as $1/N_s$. For $N_s = 8$, 12, and 16 this trend is not seen here. This is especially obvious for the case $r = 1$ where, as we

discussed in the first paragraph of this section, the gap remains relatively unchanged.

Since the ground state resembles a filled Fermi sea, it is reasonable to apply the conventional techniques in 1D physics, which deals with a perturbation expansion starting from the Fermi sea, to the present problem. The lowest order diagrams for the two-particle vertex functions at momentum transfer $2k_F$ are illustrated in Fig. 3. For an ordinary 1D spinless electron gas, there is usually a cancellation between the Cooper [(a)–(d)] and zero sound channel [(e)–(h)] instabilities so that the CDW instability does not occur.[5] As we have emphasized in section II, the matrix element A that enters into these diagrams have a more complicated momentum dependence than the conventional 1D models. The scattering amplitudes corresponding to Figs. 3(a), 3(b) and 3(c), 3(d), 3(e), 3(f) and 3(g), 3(h) are, respectively,

$$\int dq_3 A(2k_F+q_3,q_3) A(2k_F+q_3,q_3)\theta(q_3>0)/(2\pi v q_3),$$

$$\int dq_3 A(2k_F+q_3,q_3) A(q_3,q_3+2k_F)\theta(q_3>0)/(2\pi v q_3),$$

$$\int dq_3 A(q_3,2k_F+q_3) A(q_3,2k_F+q_3)\theta(q_3>0)/(2\pi v q_3),$$

$$\int dq_3 A(2k_F,q_3)^2\theta(q_3>0)/(2\pi v q_3),$$

$$\int dq_3 A(2k_F,q_3) A(q_3,q_3+2k_F)\theta(q_3>0)/(2\pi v q_3),$$

$$\int dq_3 A(q_3,2k_F) A(q_3,2k_F)\theta(q_3>0)/(2\pi v q_3).$$

In the conventional 1D RG calculation, there is a cancellation of the scattering amplitudes between the Cooper and the zero sound channel. In the present case because of the momentum dependence of the matrix elements the cancellation between these two types of terms becomes incomplete. However, the incomplete cancellation only provides for nonlogarithmic correction in the second-order diagram here. This comes about because the infrared divergence arises when the energy denominator q_3 is zero and the matrix elements cancel at and only at $q_3=0$. Expanding the matrix elements about $q_3=0$ by a linear extrapolation as

$$A(x,2k_F+y)=(|x| A_1+yA_2+1)A(0,2k_F),$$

the sum of 3(d) and 3(h) becomes $2A_2g^2k_F/2\pi v$. In general, this incomplete cancellation provides for logarithmic corrections of the order $A^n[\ln(k/k_F)]^{n-1}$ in the nth order diagram. To illustrate, let us look at the third order diagrams.

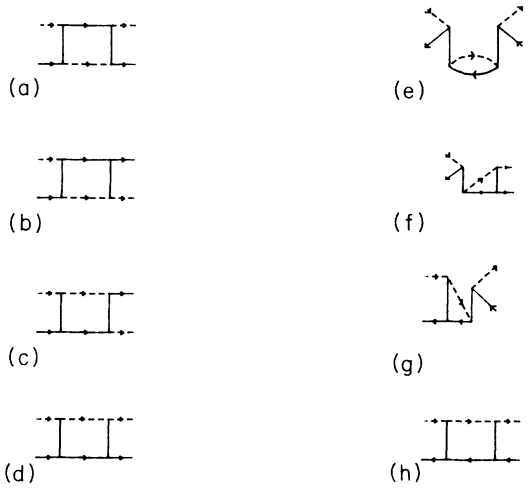

FIG. 3. Second order vertex diagrams (a)–(d) Cooper channels and (e)–(h), zero-sound channel. An electron near $+k_F$ ($-k_F$) is denoted by a solid (dashed) line.

The most important and relevant cancellation involves only g_2 because the initial value of g_2 is much bigger than g_1. The conventional first-order RG equations are given by

$$g_1'=g_1^2/(2\pi v),$$

$$g_2'=g_1^2/(2\pi v),$$

where the prime denotes differentiation with respect to $x=\ln\omega/E_F$. The solution is given by $g_1(x)=g_1(0)/[1-xg_1(0)]$, $g_2(x)=g_2(0)-g_1(0)+g_1(x)$. For an initial $g_1(0)$ that is positive, $g_1(x)$ scales to zero and g_2 scales to $g_2(0)-g_1(0)$ as x approaches $-\infty$. There are no terms on the right-hand side of the RG equations proportional to only g_2. Any new term that involves only g_2 will break this "symmetry". The higher power term that is proportional to g_1 on the right-hand side will only scale to zero and will not change the scaling trajectories discovered in the first-order RG calculation ignoring the cancellation. The only third-order diagrams that involve g_2 alone corresponds to six ladder-type diagrams with different combinations of particle or hole intermediate states. Two typical ones that correspond to all particle-particle and all particle-hole intermediate states are shown in Fig. 4. The corresponding scattering amplitudes are:

$$\int dq_3dq_4 A(q_3,2k_F) A(-q_3+q_4,2k_F) A(q_4,2k_F)\theta(q_3>0)\theta(q_4>0)/(4\pi^2v^2q_3q_4),$$

$$\int dq_3dq_4 A(q_3,2k_F+q_3) A(-q_3+q_4,2k_F+q_3+q_4) A(q_4,2k_F+q_4)\theta(q_3>0)\theta(q_4>0)/(4\pi^2v^2q_3q_4).$$

The other four involve the same energy denominator but are different in sign. They involve the matrix elements

$$A(q_3,2k_F+q_3-q_4) A(-q_3+q_4,2k_F+q_3) A(q_4,2k_F)\theta(q_4<q_3),$$

$$A(q_3,2k_F+q_4) A(-q_3+q_4,2k_F+q_4) A(q_4,2k_F+q_4)\theta(q_4<q_3),$$

$$A(q_3,2k_F) A(-q_3+q_4,2k_F+q_4) A(q_4,2k_F+q_4-q_3)\theta(q_4>q_3),$$

and

$$A(q_3,2k_F+q_3) A(-q_3+q_4,2k_F+q_3) A(q_4,2k_F+q_3)\theta(q_4>q_3).$$

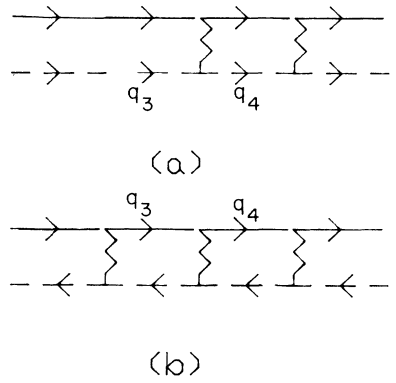

FIG. 4. Third-order vertex diagrams (a) Cooper channels and (b) zero-sound channel that involve g_2 alone. An electron near $+k_F$ ($-k_F$) is denoted by a solid (dashed) line.

We shall approximate the matrix elements by a linear extrapolation as

$$A(x,2k_F+y)=(\,|x|\,A_1+yA_2+1)A(0,2k_F).$$

The difference between the above scattering elements thus becomes

$$-A(0,2k_F)^3A_2k_F\ln(\omega/E_F)/(\pi^2v^2)\ .$$

Different guesses can be made as to the nature of the scaling relationships as a consequence of this incomplete cancellation. These guesses lead to different RG equations even though the results are qualitatively similar. We shall be guided by the higher-order terms of the perturbation expansion for the two-particle vertex in picking the scaling relationship. It is not difficult to see that the nth order term of the vertex function is equal to

$$2n[A(0,2k_F)/(2\pi v)]^nA_2k_F\ln^{n-1}(\omega/E_F).$$

We thus expect that g_2 can be expressed in terms of an auxillary coupling f such that $g(x)=2A_2k_F\partial_x f$, $x=\ln(\omega/E_F)$ and that f satisfies the RG equation

$$f'=-f^2/2\pi v$$

with the solution $f(x)=f(0)/[1+xf(0)/2\pi v]$. Hence as x goes to $-\infty$, f and hence g_2 goes to ∞.

To understand the significance of our scaling assumption, we have examined another possible guess which is consistent with the third-order terms but not with the higher-order term of the expansion for the two particle vertex. Specifically, we try to incorporate the third-order result in a second-order RG calculation. The resulting equation is then integrated numerically. In this calculation, the effect of the g_2 term is smaller; the critical value x_c at which g_2 approaches ∞ is more negative. Even though this assumption is inaccurate, the scaling trajectory is similar to that obtained above. This result illustrates the "universality" of the extra g_2 term and the irrelevance of the g_1 terms in the presence of the g_2 term in the RG equation.

To gain more confidence on the size dependence of our result, we have performed *self-consistent* numerical calculations for the eight electrons with $N_s=16$. To perform the calculation we have restricted the basis states to those with less than four clusters. The resulting ground and low-lying excited states wave function are then examined and are found to exhibit small fluctuations about the single cluster configuration. Hence our calculation is self-consistent. The case with $r=1$ exhibits a larger fluctuation; for $L_x=4.76$, the gap changes from 0.24 to 0.26.

To gain more insight into the narrow channel situation, we investigate a limiting case such that the channel width is much smaller than the magnetic length. The physics is expected to approach the zero magnetic field limit. In that case the wave function approaches the form $\sin(\pi x/d)\exp(iky)$ with eigenvalues equal to $(\hbar^2/2m)[(\pi/a)^2+d^2/12+k^2]$. We have looked at a case with a width equal to $\frac{1}{3}$. Both the eigenvalue and the eigenfunction obtained from the numerical solution of the Schrödinger equation are found to agree well with the approximate analytic results. Using these, we have diagonalized the Hamiltonian with 12 states for $r=1$. We do not find any evidence of a gap. The seperation between the ground state ($J=39$) and the first excited state ($J=40$) is equal to 0.02. Because the wave function maintains the same x dependence as k is changed in the present case, the overlap of the wave function in the x direction does not decrease as k is increased. The exchange contribution to the matrix element A exhibits a different k dependence from what we have discussed. The incomplete cancellation between the Cooper and the CDW channel mentioned in the preceding section is absent in the present case. From this point of view, the absence of a gap is reasonable.

IV. TRANSITION TO 2D BEHAVIOR

Normally the direct Coulomb interaction keeps the electrons away from each other. The clustering tendency in the ground state seems to come from the multiparticle exchange. The diagonal term of the Hamiltonian in Eq. (3) is the difference of the direct and the exchange contribution. At small distances k, these two contributions are comparable in magnitude; the net value of V is reduced, V is attractive. As k increases, the exchange contribution dies off exponentially fast and only the direct contribution remains. The distance l_t at which V turns from attractive to repulsive in units of the magnetic length is fixed. This is shown in Fig. 5 for $N_s=16$. It is because of the attractive exchange part of V that the particles form clusters. For $L_x<l_t$, a one-cluster configuration is stable. As L_x is increased, there will be a competition between the one- and the two-cluster configurations and eventually the ground state becomes the two-cluster configuration. In this way more and more clusters will be formed.

To investigate this, we have performed calculations for $L_x=4.76,6.73,8.237,9.51,10.25$. The gap as a function of L_x is shown in Fig. 6. As L_x is increased from 4.76, the gap goes towards zero because of the competition and fluctuation between the one- and two-cluster configurations. As L_x is increased further, the gap increases back up.

For $N_s=16$, the ground state at small L_x corresponds

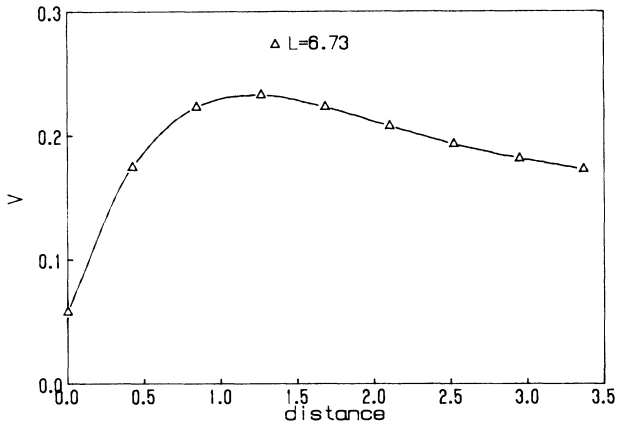

FIG. 5. The diagonal interaction $V(4,k)$ [Eq. (5)] between the particles for a system with $N_s=16$. The distance is expressed in units of the magnetic length.

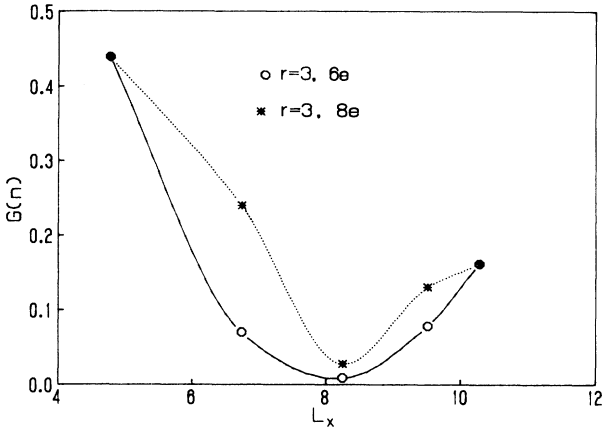

FIG. 6. The gap as a function of the channel width for six-particle and eight-particle systems. $r=3$.

to the single cluster configuration [5,6,7,8,9,10,11,12] with $J=68$. For $L_x=10.25$, the ground state corresponds to the two cluster configuration [3,4,5,9,10,11,12,13] with $J=67$. The energy difference of these two states as a function of L_x is equal to 0.418, 0.238, −0.027, −0.16, −0.16 for $L_x=4.76,6.73,8.23,9.51,10.25$ respectively. This illustrates the crossover from the one-cluster to the two-cluster configuration.

The calculation for the $N_s=16$ case was carried out under the approximation of retaining those basis states with less than or equal to four clusters. To get an idea of the validity of the approximation, consider the worst case of a small gap situation at $L_x=8.23$. The lowest wave function at $J=67$ is concentrated at

$$-0.88\,|\,3,4,5,9,10,11,12,13\rangle+0.355\,|\,3,4,6,8,10,11,12,13\rangle$$
$$-0.149\,|\,3,4,7,8,9,11,12,13\rangle-0.203\,|\,3,5,6,7,10,11,12,13\rangle+0.135\,|\,2,4,6,9,10,11,12,13\rangle.$$

The rest of the amplitudes are much smaller. After one hop from the two cluster ground-state configuration, the amplitude has come down by an average of 30%. The states that we have discarded can be reached from the two cluster configuration by at least two hops. In addition, its energy is much higher. Thus our approximation is quite good. Note that the second state can be obtained from the first state via the excitation 5 to 8 and 9 to 6. Similarly, the third corresponds to the excitation 5 to 8 and 10 to 7; the fourth corresponds to 4 to 7 and 9 to 6, while the last corresponds to 5 to 2 and 3 to 6. The momentum transfer of these processes is 3 and is approximately equal to $2k_F$ for a single cluster. The last one corresponds to an intracluster excitation while the remaining ones correspond to intercluster excitations. The physical picture in this case seems to correspond to a triangular "lattice" with two rows in the x direction. The origin of the commensuration seems to come from exchange, however.

Because of finite size crossover effects, there is large fluctuation in the magnitude of the gap as the sample size is changed at intermediate values of L_x. For example, at $L_x=6.73$, the ground state for $N_s=12$ corresponds to a two cluster configuration [4,5,6,8,9,10] already whereas for $N_s=16$ the ground state is still a single cluster configuration. This is why the gap value is so different for $N_s=12$ and 16 for $L_x=6.73$.

From these calculations we estimate the gap to be equal to 0.16 at $L_x=10.25$. For $N_s=16$, the first excited state occurs at $J=64$ and is dominated by the configuration [3,4,5,6,10,11,12,13] with a bare energy 4.35. The ground-state configuration [3,4,5,9,10,11,12,13] has an energy 4.14. The difference of these two bare energies, 0.16, is very close to the magnitude of the gap. While we believe the difference of the diagonal energies provides for an estimate of the gap, we consider the degree of agreement obtained in this case to be fortuitous because of the fluctuations about these configurations.

In the calculation that we have performed, the configurations with different numbers of clusters possess different total y momenta J and hence are not coupled to each other. This is characteristic of the even-denominator situation. As the transverse dimension is increased, the fluctuation in the number of clusters eventually destroys the gap. There are situations such that configurations with different numbers of clusters occur with the same J and hence are coupled to each other. A gap is produced due to the hybridization of these local minima. This is characteristic of the bulk limit odd-denominator situation. To bring the matter into perspective and to make our discussion of the FQHE ground state more concrete, we provide here the explicit ground-state wave function for the FQHE for a case with $N_s=12$, 1/3 filled, $J=10$, and aspect ratio equal to 1, periodic BC was used. This represents nothing new numerically, but the simplicity of

the wave function does not seem to have been appreciated previously. The ground state is dominated by the three cluster configuration. More precisely, for an aspect ratio of 1, the ground state is dominated by configurations of 1 cluster of 2 and 2 clusters of 1 with probability density of 0.568 $[0.377(|1,4,8,9\rangle+|1,5,6,10\rangle+|2,3,7,10\rangle-|4,7,11,12\rangle)]$, of 2 clusters of 2 with probability density 0.191 $[0.3088(|5,6,11,12\rangle-|2,3,8,9\rangle)]$, of 4 clusters of 1 equally spaced at distance 2 apart with probability density 0.09 $[-0.302|1,4,7,10\rangle]$ and 4 clusters of 1 but spaced at distances 3,3,1,1 with probability density 0.13 $[-0.182(|1,5,7,9\rangle+|2,4,6,10\rangle-|4,8,10,12\rangle-|1,3,7,11\rangle)]$. (The total sum of these probability densities adds up to 0.979). The first excited state corresponds to the ground state at $J=9$. It is approximately equal to $\rho(qy=1,qx=\pi/3)|0\rangle$ after proper normalization.

TABLE I. The gap Δ at half filled and one-third filled as a function of the transverse length L_y.

L_y	4.3	7.1	7.7	8.7	∞
$\Delta(\frac{1}{2})$	0.31	0	0.05	0.07	0
$\Delta(\frac{1}{3})$	0.15	0.075	0.08	0.08	0.06

$$[0.335(|1,5,6,9\rangle-|2,3,6,10\rangle-|3,7,11,12\rangle+|4,8,9,12\rangle)$$
$$+0.247(-|1,3,7,10\rangle+|1,4,6,10\rangle-|1,4,7,9\rangle-|4,7,10,12\rangle)$$
$$+0.23(|1,3,8,9\rangle+|2,3,7,9\rangle+|4,6,11,12\rangle+5,6,10,12\rangle)$$
$$+0.109(-|1,3,6,11\rangle+|5,7,9,12\rangle-|2,4,6,9\rangle)].$$

For free boundary conditions in a finite channel, configurations with different clusters may still occur at the same J at particular filling factors. In general, this will no longer be exactly $\frac{1}{3}$ and will be very hard to determine numerically. To illustrate the difference between the odd and the even denominator situations, we shall thus confine our interest to the case of periodic boundary conditions where the commensuration conditions occur exactly at $\frac{1}{3}$. In that case the particle can never move outside the channel; if it goes out on one side, it comes back on the other. Our results with the y axis across the channel are summarized in Table I for a 12 site situation. For $L_y=4.3,7.1,7.7,8.7$, the gap at half-filled oscillates and is equal to 0.31, 0, 0.05, and 0.07 respectively, whereas at one-third-filled, the gap is equal to 0.15, 0.075, 0.08, and 0.08, respectively, and is never close to zero. From calculations using the computer RG technique with systematic truncation that we have described previously[10] we get gaps equal to 0.11 and 0 for $L_y=8.7,7.1$ for 24 site clusters at half-filled, consistent with the 12 site results. For $L_y=8.7$ and $N_s=12$, the static structure factor $S(q,0)$ for the ground state possesses a peak of magnitude 1.3 at $q=2\pi/6a$ where a is the intersite spacing, indicating the formation of the "cluster" distribution with three contiguous sites occupied and then three empty sites next to it. For large q, $S(q,0)$ approaches 1. For other values of J, we do not see any peak in the structure factor. The magnitude of this peak for the 12 site case is similar to that from finite cluster calculations at one-third filled.

We next turn our attention to the question of ground-state degeneracy. For the 2D FQHE under periodic boundary conditions, states with J's whose difference is modulo N_s are coupled together, there is a ν fold center of mass degeneracy of the ground state at filling factor $1/\nu$. In the present case, states with J's whose difference is modulo N_s is considered different, we expect this degeneracy to be of the order of L_y.

Experimentally the width of a channel is never uniform. Thus there will be regions where there is a gap and regions where there is no gap if the fluctuation in the width gets large enough. However ρ_{xx} for the whole channel will still be zero in the idealized situation.

ACKNOWLEDGMENT

I thank K. B. Ma for helpful discussions.

[1]D. C. Tsui, H. L. Stormer, and A. C. Gossard, Phys. Rev. Lett. **48**, 1559 (1982); H. L. Stormer *et al.*, *ibid.* **50**, 1953 (1983).

[2]Surf. Sci. **142**, (1984).

[3]S. T. Chui, Phys. Rev. Lett. **56**, 2395 (1986).

[4]S. T. Chui, Phys. Rev. B **32**, 8438 (1985).

[5]Yu. A. Bychkov, L. P. Gorkov, and I. Dzyaloshinskii, Zh. Eksp. Teor. Fiz. **50**, 738 (1966) [JETP **23**, 489 (1966)]; N. Menyhard and J. Solyom, J. Low Temp. Phys. **12**, 529 (1973); A. Luther and V. Emery, Phys. Rev. Lett. **33**, 589 (1974); S. T. Chui and P. A. Lee, *ibid.* **35**, 315 (1975); S. T. Chui, T. M. Rice, and C. M. Varma, Solid State Commun. **15**, 155 (1974).

[6]E. Tosatti and M. Parrinello, Lett. Nuovo Cimento **36**, 289 (1983); S. Kivelson, C. Kallen, D. P. Arovas, and J. R. Schrieffer, Phys. Rev. Lett. **56**, 873 (1986); S. T. Chui, Phys. Rev. B **34**, 1130 (1986).

[7]Here, distances have been expressed in units of the magnetic length and would continue to be so in the rest of this paper.

[8]P. M. Morse and H. Feshbach, *Methods of Theoretical Physics* (McGraw Hill, New York, 1953), Vol. 2, p. 1403.

[9]For $j_y=0$, the sum over p is infinite in the limit r goes to zero for finite N_s. This term is a finite-size effect. It does not affect the excitation spectrum and will be zero in the limit that L_y and hence N_s approaches infinity. Thus this term has been subtracted off.

[10]S. T. Chui, Phys. Rev. B **32**, 1436 (1985).